

The Impact of an Extra Background of Relativistic Particles on the Cosmological Parameters derived from Microwave Background Anisotropies

Rebecca Bowen¹, Steen H. Hansen¹, Alessandro Melchiorri¹, Joseph Silk¹,
Roberto Trotta²

¹ *Nuclear and Astrophysics Laboratory, University of Oxford, Keble Road, Oxford, OX 3RH, UK*

² *Département de Physique Théorique, Université de Genève, 24 quai Ernest Ansermet, CH-1211 Genève 4, Switzerland*

24 October 2018

ABSTRACT

Recent estimates of cosmological parameters derived from Cosmic Microwave Background (CMB) anisotropies are based on the assumption that we know the precise amount of energy density in relativistic particles in the universe, ω_{rel} , at all times. There are, however, many possible mechanisms that can undermine this assumption. In this paper we investigate the effect that removing this assumption has on the determination of the various cosmological parameters. We obtain fairly general bounds on the redshift of equality, $z_{eq} = \omega_m/\omega_{rel} = 3100^{+600}_{-400}$. We show that ω_{rel} is nearly degenerate with the amount of energy in matter, ω_m , and that its inclusion in CMB parameter estimation also affects the present constraints on other parameters such as the curvature or the scalar spectral index of primordial fluctuations. This degeneracy has the effect of limiting the precision of parameter estimation from the MAP satellite, but it can be broken by measurements on smaller scales such as those provided by the Planck satellite mission.

Key words: cosmology: cosmic microwave background, cosmological parameters

1 INTRODUCTION

Our knowledge of the cosmological parameters has increased dramatically with the release of recent cosmic microwave background (CMB) observations (Netterfield et al. 2001; Lee et al. 2001; Halverson et al. 2001). Recent analyses of these datasets (de Bernardis et al. 2001; Pryke et al. 2001; Wang, Tegmark & Zaldarriaga 2001) have reported strong new constraints on various parameters including the curvature of the universe and the amount of baryonic and dark matter. The precise determination from the CMB of other parameters such as the cosmological constant or the spectral index of primordial fluctuations can be limited by various degeneracies, and such degeneracies are best lifted by combining CMB data with either supernova (SN) data (Garnavich et al. 1998; Perlmutter et al. 1997) or large scale structure (LSS) surveys, such as PSCz (Saunders et al. 2000), 2dF (Percival et al. 2001) or Lyman- α (Croft et al. 2001) data. At present, the values obtained from CMB measurements under the assumption of purely adiabatic fluctuations are consistent with the generic predictions of the inflationary scenario, $n_s \sim 1$ and $\Omega_{tot} = 1$ (Linde 1990), and with the standard big-bang nucleosynthesis bound, $\Omega_b h^2 = 0.020 \pm 0.002$ (Burles et al. 2001; Esposito et al. 2001). All of these observations con-

verge towards a consistent picture of our universe, providing strong support for the inflationary scenario as the mechanism which generated the initial conditions for structure formation.

The derivation of the cosmological parameters from CMB is, however, an *indirect* measurement, relying on the assumptions of a theoretical scenario. For this reason, recent efforts have been made to study the effects of the removal of some of these assumptions. For example, a scale-invariant background of gravity waves, generally expected to be small, has been included in the analysis of Kinney, Melchiorri & Riotto (2000), Wang et al. (2001) and Efstathiou et al. (2001), with important consequences for parameter estimation. A scale-dependence of the spectral index has been included in the analysis of Griffiths, Silk & Zaroubi (2001), Santos et al. (2001) and Hannestad et al. (2001). Furthermore, in Bucher, Moodley & Turok (2000), Trotta, Riazuelo & Durrer (2001) and Amendola et al. (2001), the effects of including isocurvature modes, which naturally arise in the most general inflationary scenarios, have been studied, with the finding that the inclusion of these modes can significantly alter the CMB result. Even more drastic alterations have been proposed in Bouchet et al. (2001) and Durrer, Kunz & Melchiorri (2001).

All the above modifications primarily affect the con-

straints on the curvature, on the physical baryon density parameter, $\omega_b = \Omega_b h^2$, and the scalar spectral index n_s .

In this paper we study another possible modification to the standard scenario, namely variations in the parameter ω_{rel} which describes the energy density of relativistic particles at times near decoupling, $T \sim 0.1$ eV. CMB data analysis with variations in this parameter has been recently undertaken by many authors (Hannestad 2000; Esposito et al. 2001; Orito et al. 2001; Hansen et al. 2001; Kneller et al. 2001; Hannestad 2001; Zentner & Walker 2001), giving rather crude upper bounds, significantly improved only by including priors on the age of the universe or by including supernovae (SN) or large scale structure (LSS) data. It is worth emphasizing that there is little difference in the bounds obtained on N_{eff} , the effective number of relativistic species, between old and recent CMB data because of the degeneracy which we will describe in detail below. We focus here on the effects that the inclusion of this parameter, ω_{rel} , has on the constraints of the remaining parameters in the context of purely adiabatic models.

As we will show below (and as observed previously, see e.g. Hu et al. (1999)) there is a strong degeneracy between ω_{rel} and ω_m . This is important, because an accurate determination of ω_m from CMB observations (and of Ω_m by including the Hubble Space Telescope result $h = 0.72 \pm 0.08$) can be useful for a large number of reasons. First of all, determining $\omega_{cdm} = \omega_m - \omega_b$ can shed new light on the nature of dark matter. The thermally averaged product of cross-section and thermal velocity of the dark matter candidate is related to ω_m , and this relation can be used to analyze the implications for the mass spectra in versions of the Supersymmetric Standard Model (see e.g. Barger & Kao 2001, Djouadi, Drees & Kneur 2001, Ellis, Nanopoulos & Olive 2001). The value of Ω_m can be determined in an independent way from the mass-to-light ratios of clusters (Turner 2001), and the present value is $0.1 < \Omega_m < 0.2$ (Carlberg et al. 1997; Bahcall et al. 2000). Furthermore, a precise measurement of Ω_m will be a key input for determining the redshift evolution of the equation of state parameter $w(z)$ and thus discriminating between different quintessential scenarios (see e.g. Weller and Albrecht 2001).

This paper is structured as follows. In the next section, we briefly review various physical mechanisms that can lead to a change in ω_{rel} with respect to the standard value. In section 3, we illustrate how the CMB angular power spectrum depends on this parameter and identify possible degeneracies with other parameters. In section 4, we present a likelihood analysis from the most recent CMB data and show which of the present constraints on the various parameters are affected by variations in ω_{rel} . Section 5 forecasts the precision in the estimation of cosmological parameters for the future space missions MAP and Planck. Finally, in section 6, we discuss our results and present our conclusions.

2 EFFECTIVE NUMBER OF RELATIVISTIC SPECIES

In the standard model ω_{rel} includes photons and neutrinos, and it can be expressed as

$$\omega_{rel} = \omega_\gamma + N_{eff} \cdot \omega_\nu \quad (1)$$

where ω_γ is the energy density in photons and ω_ν is the energy density in one active neutrino. Measuring ω_{rel} thus gives a direct observation on the effective number of neutrinos, N_{eff} . Naturally there are only 3 active neutrinos, and N_{eff} is simply a convenient parametrization for the extra possible relativistic degrees of freedom

$$N_{eff} = 3 + \Delta N_{CMB}. \quad (2)$$

Thus ω_{rel} includes energy density from all the relativistic particles: photons, neutrinos, and additional hypothetical relativistic particles such as a light majoron or a sterile neutrino. Such hypothetical particles are strongly constrained from standard big bang nucleosynthesis (BBN), where the allowed extra relativistic degrees of freedom typically are expressed through the effective number of neutrinos, $N_{eff} = 3 + \Delta N_{BBN}$. BBN bounds are typically about $\Delta N_{BBN} < 0.2 - 1.0$ (Burles et al. 1999; Lisi, Sarkar & Villante 1999).

One should, however, be careful when comparing the effective number of neutrino degrees of freedom at the times of BBN and CMBR, since they may be related by different physics (Hansen et al. 2001). This is because the energy density in relativistic species may change from the time of BBN ($T \sim$ MeV) to the time of last rescattering ($T \sim$ eV). For instance, if one of the active neutrinos has a mass in the range $eV < m < \text{MeV}$ and decays into sterile particles such as other neutrinos, majorons etc. with lifetime $t(\text{BBN}) < \tau < t(\text{CMBR})$, then the effective number of neutrinos at CMBR would be substantially different from the number at BBN (White, Gelmini & Silk 1995). Such massive active neutrinos, however, do not look too natural any longer in view of the recent experimental results on neutrino oscillations (Fogli et al. 2001; Gonzalez-Garcia et al. 2001), showing that all active neutrinos are likely to have masses smaller than an eV. One could instead consider sterile neutrinos mixed with active ones which could be produced in the early universe by scattering, and subsequently decay. The mixing angle must then be large enough to thermalize the sterile neutrinos (Langacker 1989), and this can be expressed through the sterile to active neutrino number density ratio $n_s/n_\nu \approx 4 \cdot 10^4 \sin^2 2\theta (m/\text{keV})(10.75/g^*)^{3/2}$ (Dolgov & Hansen 2001), where θ is the mixing angle, and g^* counts the relativistic degrees of freedom. With n_s/n_ν of order unity we use the decay time, $\tau \approx 10^{20} (\text{keV}/m)^5 / \sin^2 2\theta$ sec, and one finds, $\tau \approx 10^{17} (\text{keV}/m)^4 \text{yr}$, which is much longer than the age of the universe for $m \sim \text{keV}$, so they would certainly not have decayed at $t(\text{CMBR})$. A sterile neutrino with mass of a few MeV would seem to have the right decay time, $\tau \sim 10^5 \text{yr}$, but this is excluded by standard BBN considerations (Kolb et al. 1991; Dolgov, Hansen & Semikoz 1998).

Even though the simplest models predict that the relativistic degrees of freedom are the same at BBN and CMB times, one could imagine more inventive models such as quintessence (Albrecht & Skordis 2000; Skordis & Albrecht 2001) which effectively could change ΔN between BBN and CMB (Bean, Hansen & Melchiorri 2001). Naturally ΔN can be both positive and negative. For BBN, ΔN can be negative if the electron neutrinos have a non-zero chemical potential (Kang & Steigman 1992; Kneller et al. 2001), or more generally with a non-equilibrium electron neutrino distribution function (see e.g. Hansen & Villante 2000). To give an

explicit (but highly exotic) example of a different number of relativistic degrees of freedom between BBN and CMB, one could consider the following scenario. Imagine another 2 sterile neutrinos, one of which is essentially massless and has a mixing angle with any of the active neutrinos just big enough to bring it into equilibrium in the early universe, and one with a mass of $m_{\nu_s} = 3$ MeV and decay time $\tau_{\nu_s} = 0.1$ sec, in the decay channel $\nu_s \rightarrow \nu_e + \phi$, with ϕ a light scalar. The resulting non-equilibrium electron neutrinos happen to exactly cancel the effect of the massless sterile state, and hence we have $\Delta N_{BBN} = 0$. However, for CMB the picture is much simpler, and we have just the stable sterile state and the majoron, hence $\Delta N_{CMB} = 1.57$. For CMB, one can imagine a negative ΔN from decaying particles, where the decay products are photons or electron/positrons which essentially increases the photon temperature relative to the neutrino temperature (Kaplinghat & Turner 2001). Such a scenario naturally also dilutes the baryon density, and the agreement on ω_b from BBN and CMB gives a bound on how negative ΔN_{CMB} can be. Considering all these possibilities, we will therefore not make the usual assumption, $\Delta N_{BBN} = \Delta N_{CMB}$, but instead consider ΔN_{CMB} as a completely free parameter in the following analysis.

The standard model value for N_{eff} with 3 active neutrinos is 3.044. This small correction arises from the combination of two effects arising around the temperature $T \sim$ MeV. These effects are the finite temperature QED correction to the energy density of the electromagnetic plasma (Heckler 1994), which gives $\Delta N = 0.01$ (Lopez & Turner 1999; Lopez et al. 1999). If there are more relativistic species than active neutrinos, then this effect will be correspondingly higher (Steigman 2001). The other effect comes from neutrinos sharing in the energy density of the annihilating electrons (Dicus et al. 1982), which gives $\Delta N = 0.034$ (Dolgov, Hansen & Semikoz 1997, 1999; Esposito et al. 2000). Thus one finds $N_{eff} = 3.044$. It still remains to accurately calculate these two effects simultaneously.

3 CMB THEORY AND DEGENERACIES

The structure of the C_ℓ spectrum depends essentially on 4 cosmological parameters

$$\omega_b, \omega_m, \omega_{rel} \text{ and } \mathcal{R}, \quad (3)$$

the physical baryonic density $\omega_b \equiv \Omega_b h^2$, the energy density in matter $\omega_m \equiv (\Omega_{cdm} + \Omega_b) h^2$, the energy density in radiation ω_{rel} and the ‘shift’ parameter $\mathcal{R} \equiv \ell_{ref}/\ell$, which gives the position of the acoustic peaks with respect to a flat, $\Omega_\Lambda = 0$ reference model. Here h denotes the Hubble parameter today, $H_0 \equiv 100h$ km s⁻¹ Mpc⁻¹, and Ω_Λ is the density parameter due to a cosmological constant, $\Omega_\Lambda \equiv \Lambda/3H_0^2$. In previous analyses (Efstathiou & Bond 1999; Melchiorri & Griffiths 2000 and references therein), the parameter ω_{rel} has been kept fixed to the standard value, while here we will allow it to vary. It is therefore convenient to write $\omega_{rel} = 4.13 \cdot 10^{-5} (1 + 0.135 \cdot \Delta N)$ (taking $T_{CMB} = 2.726$ K), where ΔN is the excess number of relativistic species with respect to the standard model, $N_{eff} = 3 + \Delta N$. The shift parameter \mathcal{R} depends on $\Omega_m \equiv \Omega_{cdm} + \Omega_b$, on the curvature Ω_k and on $\Omega_{rel} = \omega_{rel}/h^2$ through

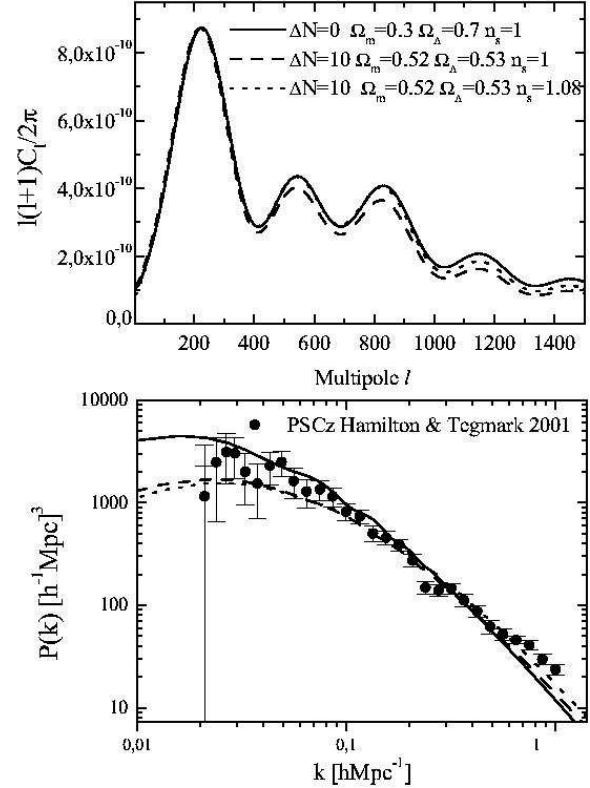


FIG. 1 — Top panel: CMB degeneracies between cosmological models. Keeping z_{eq}, ω_b and \mathcal{R} fixed while varying ΔN produces nearly degenerate power spectra. The reference model (black, solid) has $\Delta N = 0, \Omega_{tot} = 1.00, n_s = 1.00$; the nearly degenerate model (blue, dotted) has $\Delta N = 10, \Omega_{tot} = 1.05, n_s = 1.00$. The position of the peaks is perfectly matched, only the relative height between the first and the other acoustic peaks is somewhat different in this extreme example. The degeneracy can be further improved, at least up to the third peak, by raising the spectral index to $n_s = 1.08$ (red, dashed). Bottom panel: the matter power spectra of the models plotted in the top panel together with the observed decorrelated power spectrum from the PSCz survey (Hamilton and Tegmark 2000). The geometrical degeneracy is now lifted.

$$\mathcal{R} = 2 \left(1 - \frac{1}{\sqrt{1 + z_{dec}}} \right) \times \frac{\sqrt{|\Omega_k|}}{\Omega_m} \frac{1}{\chi(y)} \left[\sqrt{\Omega_{rel} + \frac{\Omega_m}{1 + z_{dec}}} - \sqrt{\Omega_{rel}} \right], \quad (4)$$

where

$$y = \sqrt{|\Omega_k|} \int_0^{z_{dec}} dz \quad (5)$$

$$[\Omega_{rel}(1+z)^4 + \Omega_m(1+z)^3 + \Omega_k(1+z)^2 + \Omega_\Lambda]^{-1/2}.$$

The function $\chi(y)$ depends on the curvature of the universe and is $y, \sin(y)$ or $\sinh(y)$ for flat, closed or open models, respectively. Eq. (4) generalizes the expression for \mathcal{R} given in Melchiorri & Griffiths (2001) to the case of non-constant Ω_{rel} .

By fixing the 4 parameters given in (3), or equivalently the set ω_b , the redshift of equality $z_{eq} \equiv \omega_m/\omega_{rel}$, ΔN and

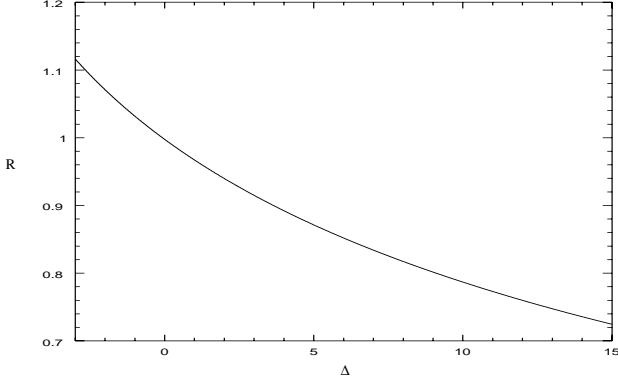


FIG. 2.— \mathcal{R} as a function of ΔN with $\Omega_\Lambda = 0.7$ and $\Omega_m = 0.3$. The position of the peaks is only weakly affected by ΔN .

\mathcal{R} , one obtains a perfect degeneracy for the CMB anisotropy power spectra on degree and sub-degree angular scales. On larger angular scales, the degeneracy is broken by the late Integrated Sachs-Wolfe (ISW) effect because of the different curvature and cosmological constant content of the models. From the practical point of view, however, it is still very difficult to break the degeneracy, since measurements are limited by ‘‘cosmic variance’’ on those scales, and because of the possible contribution of gravitational waves.

Allowing ΔN to vary, but keeping constant the other 3 parameters ω_b , z_{eq} , and \mathcal{R} , we obtain nearly degenerate power spectra which we plot in Fig. 1, normalized to the first acoustic peak. The degeneracy in the acoustic peaks region is now slightly spoiled by the variation of the ratio $\Omega_\gamma/\Omega_{rel}$: the different radiation content at decoupling induces a larger (for $\Delta N > 0$) early ISW effect, which boosts the height of the first peak with respect to the other acoustic peaks. Nevertheless, it is still impossible to distinguish between the different models with present CMB measurements and without external priors. Furthermore, a slight change in the scalar spectral index, n_s , can reproduce a perfect degeneracy up to the third peak.

The main result of this is that, even with a measurement of the first 3 peaks in the angular spectrum, it is impossible to put bounds on ω_{rel} alone, even when fixing other parameters such as ω_b . Furthermore, since the degeneracy is mainly in z_{eq} , the constraints on ω_m from CMB are also affected (see section 4).

In Fig. 2 we plot the shift parameter \mathcal{R} as a function of ΔN , while fixing $\Omega_m = 0.3$ and $\Omega_\Lambda = 0.7$. Increasing ΔN moves the peaks to smaller angular scales, even though the dependence of the shift parameter on ΔN is rather mild. In order to compensate this effect, one has to change the curvature by increasing Ω_m and Ω_Λ . We therefore conclude that the present bounds on the curvature of the universe are weakly affected by ΔN . Nevertheless, when a positive (negative) ΔN is included in the analysis, the preferred models are shifted toward closed (open) universes.

4 CMB ANALYSIS

In this section, we compare the recent CMB observations with a set of models with cosmological parameters sampled as follows: $0.1 < \Omega_m < 1.0$, $0.1 < \Omega_{rel}/\Omega_{rel}(\Delta N = 0) < 3$,

$0.015 < \Omega_b < 0.2$; $0 < \Omega_\Lambda < 1.0$ and $0.40 < h < 0.95$. We vary the spectral index of the primordial density perturbations within the range $n_s = 0.50, \dots, 1.50$ and we re-scale the fluctuation amplitude by a pre-factor C_{10} , in units of C_{10}^{COBE} . We also restrict our analysis to purely adiabatic, *flat* models ($\Omega_{tot} = 1$) and we add an external Gaussian prior on the Hubble parameter $h = 0.65 \pm 0.2$.

The theoretical models are computed using the publicly available CMBFAST program (Seljak & Zaldarriaga 1996) and are compared with the recent BOOMERanG-98, DASI and MAXIMA-1 results. The power spectra from these experiments were estimated in 19, 9 and 13 bins respectively, spanning the range $25 \leq \ell \leq 1100$. We approximate the experimental signal C_B^{ex} inside the bin to be a Gaussian variable, and we compute the corresponding theoretical value C_B^{th} by convolving the spectra computed by CMBFAST with the respective window functions. When the window functions are not available, as in the case of Boomerang-98, we use top-hat window functions. The likelihood for a given cosmological model is then defined by $-2\ln L = (C_B^{th} - C_B^{ex})M_{BB'}(C_B^{th} - C_B^{ex})$ where C_B^{th} (C_B^{ex}) is the theoretical (experimental) band power and $M_{BB'}$ is the Gaussian curvature of the likelihood matrix at the peak. We consider 10%, 4% and 4% Gaussian distributed calibration errors (in μ K) for the BOOMERanG-98, DASI and MAXIMA-1 experiments respectively. We also include the COBE data using Lloyd Knox’s RADPack packages.

In order to show the effect of the inclusion of ω_{rel} on the estimation of the other parameters, we plot likelihood contours in the $\omega_{rel} - \omega_m$, $\omega_{rel} - \omega_b$, $\omega_{rel} - n_s$ planes.

Proceeding as in Melchiorri et al. (2000), we calculate a likelihood contour in those planes by finding the remaining ‘nuisance’ parameters that maximize it. We then define our 68%, 95% and 99% confidence levels to be where the likelihood falls to 0.32, 0.05 and 0.01 of its peak value, as would be the case for a 2-dimensional Gaussian.

In Fig. 3 we plot the likelihood contours for ω_{rel} vs ω_m , ω_b and n_s (top to bottom). As we can see, ω_{rel} is very weakly constrained to be in the range $1 \leq \omega_{rel}/\omega_{rel}(\Delta N = 0) \leq 1.9$ at $1-\sigma$ in all the plots. The degeneracy between ω_{rel} and ω_m is evident in the top panel of Fig. 3. Increasing ω_{rel} shifts the epoch of equality and this can be compensated only by a corresponding increase in ω_m . It is interesting to note that even if we are restricting our analysis to flat models, the degeneracy is still there and that the bounds on ω_m are strongly affected. We find $\omega_m = 0.2 \pm 0.1$, to be compared with $\omega_m = 0.13 \pm 0.04$ when ΔN is kept to zero. It is important to realize that these bounds on ω_{rel} appear because of our prior on h and because we consider flat models. When one allows h as a free parameter and any value for Ω_m , then the degeneracy is almost complete and there are no bounds on ω_{rel} . In the middle and bottom panel of Fig. 3 we plot the likelihood contours for ω_b and n_s . As we can see, these parameters are not strongly affected by the inclusion of ω_{rel} . The bound on ω_b , in particular, is completely unaffected by ω_{rel} . There is however, a small correlation between ω_{rel} and n_s : the boost of the first peak induced by the ISW effect can be compensated (at least up to the third peak) by a small change in n_s .

Since the degeneracy is mainly in z_{eq} , it is useful to estimate the constraints we can put on this variable. In Fig. 4 we plot the likelihood contours on z_{eq} by using the marginal-

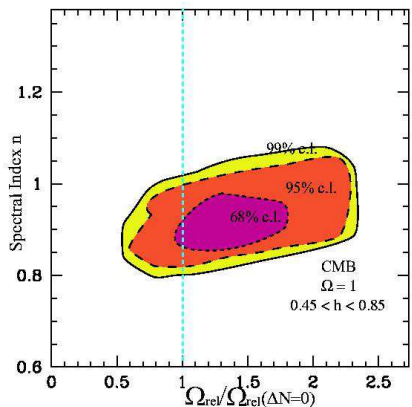
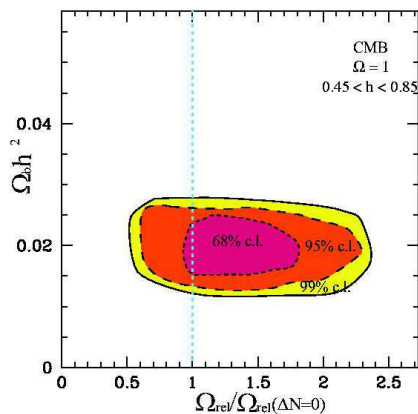
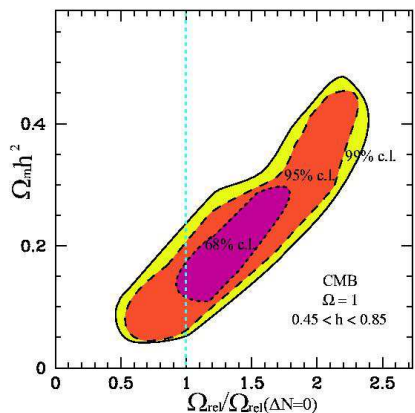


FIG. 3 — Likelihood contours plots in the $\omega_{rel} - \omega_m$, $\omega_{rel} - \omega_b$, $\omega_{rel} - n_s$ planes.

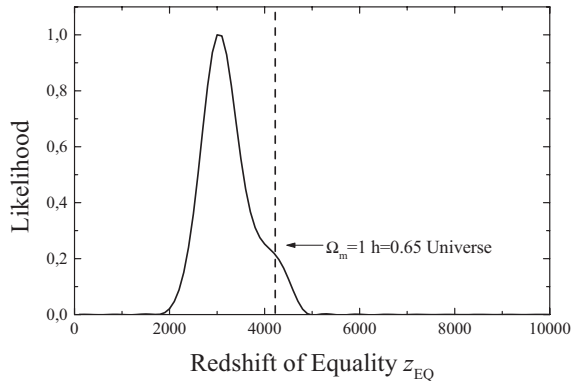


FIG. 4 — Likelihood probability distribution function for the redshift of equality.

ization/maximization algorithm described above. By integration of this probability distribution function we obtain $z_{eq} = 3100^{+600}_{-400}$ at 68% c.l., i.e. a late-time equality, in agreement with a low-density universe.

External constraints. It is interesting to investigate how well constraints from independent non-CMB datasets can break the above degeneracy between ω_{rel} and ω_m . The supernovae luminosity distance is weakly dependent on ω_{rel} (see however Zentner & Walker 2001), and the bounds obtained on Ω_m can be used to break the CMB degeneracy. Including the SN-Ia constraints on the $\Omega_m - \Omega_\Lambda$ plane, $0.8\Omega_m - 0.6\Omega_\Lambda = -0.2 \pm 0.1$ (Perlmutter et al. 1999), we find $\omega_{rel}/\omega_{rel}(\Delta N = 0) = 1.12^{0.35}_{-0.42}$ at the $2 - \sigma$ confidence level.

It is also worthwhile to include constraints from galaxy clustering and local cluster abundances. The shape of the matter power spectrum in the linear regime for galaxy clustering can be characterized by the shape parameter $\Gamma \sim \Omega_m h / \sqrt{(1 + 0.135\Delta N)e^{-\Omega_b(1 + \sqrt{2}h/\Omega_m) - 0.06}}$. From the observed data one has roughly $0.15 \leq \Gamma + (n_s - 1)/2 \leq 0.3$.

The degeneracy between ω_m and ω_{rel} in the CMB cannot be broken trivially by inclusion of large-scale structure data, because a similar degeneracy affects the LSS data as well (see e.g. Hu et al 1999). However, the geometrical degeneracy is lifted in the matter power spectrum, and accurate measurements of galaxy clustering at very large scales can distinguish between various models. This is exemplified in the bottom panel of Fig. 1, where we plot 3 matter power spectra with the same cosmological parameters as in the top panel, together with the decorrelated matter power spectrum obtained from the PSCz survey.

The inclusion of the above (conservative) value on Γ gives $\omega_{rel}/\omega_{rel}(\Delta N = 0) = 1.40^{0.49}_{-0.56}$, that is less restrictive than the one obtained with the SN-Ia prior.

A better constraint can be obtained by including a prior on the variance of matter perturbations over a sphere of size $8h^{-1}$ Mpc, derived from cluster abundance observations. Comparing with $\sigma_8 = (0.55 \pm 0.05)\Omega_m^{-0.47}$, we obtain $\omega_{rel}/\omega_{rel}(\Delta N = 0) = 1.27^{0.35}_{-0.43}$, again at the $2 - \sigma$ confidence level.

5 FORECAST FOR MAP AND PLANCK

In this section we perform a Fisher matrix analysis in order to estimate the precision with which forthcoming satellite experiments will be able to constrain the parameter z_{eq} .

Fisher matrix. Using $\mathcal{L}(\mathbf{s})$ to denote the likelihood function for the parameter set \mathbf{s} and expanding $\ln \mathcal{L}$ to quadratic order about the maximum defined by the reference model parameters \mathbf{s}_0 , one obtains

$$\mathcal{L} \approx \mathcal{L}(\mathbf{s}_0) \exp\left(-\frac{1}{2} \sum_{i,j} F_{ij} \delta s_i \delta s_j\right)$$

where the *Fisher matrix* F_{ij} is given by the expression

$$F_{ij} = \sum_{\ell}^{\ell_{max}} \frac{1}{(\Delta C_{\ell})^2} \frac{\partial C_{\ell}}{\partial s_i} \frac{\partial C_{\ell}}{\partial s_j} \quad (6)$$

and ℓ_{max} is the maximum multipole number accessible to the experiment. The quantity ΔC_{ℓ} is the standard deviation on the estimate of C_{ℓ} , which takes into account both cosmic variance and the expected error of the experimental apparatus and is given by

$$(\Delta C_{\ell})^2 \approx \frac{2}{(2\ell + 1) f_{sky}} (C_{\ell} + \bar{B}_{\ell}^{-2})^2, \quad (7)$$

$$\bar{B}_{\ell}^2 = \sum_c w_c e^{(-\ell(\ell+1)/\ell_c^2)} \quad (8)$$

(Knox 1995; Efstathiou & Bond 1999), for an experiment with N channels (denoted by a subscript c), angular resolution (FWHM) θ_c , sensitivity σ_c per resolution element and with a sky coverage f_{sky} . The inverse weight per solid angle is $w_c^{-1} \equiv (\sigma_c \theta_c)^{-2}$ and $\ell_c \equiv \sqrt{8 \ln 2} / \theta_c$ is the width of the beam, assuming a Gaussian profile. If the initial fluctuations are Gaussian and a uniform prior is assumed, one finds that the covariance matrix is given by the inverse of the Fisher matrix, $C = F^{-1}$ (Bond et al. 1997). The standard deviation for the parameter s_i (with marginalization over all other parameters) is therefore given by $\sigma_i = \sqrt{C_{ii}}$. This approximation is rigorously valid only in the vicinity of the maximum of the likelihood function, but it has proved to give useful insight even for large values of $\mathbf{s} - \mathbf{s}_0$ (Efstathiou & Bond 1999; Efstathiou 2001). The main advantage of the Fisher matrix approach when compared to an exact likelihood analysis is that for m cosmological parameters the former requires only the evaluation of $m + 1$ power spectra. Therefore the computational effort is vanishingly small with respect to the one necessary for a full likelihood analysis of the parameter space.

Table 1 summarizes the experimental parameters for MAP and Planck we have used in the analysis. For both experiment we have taken $f_{sky} = 0.50$. These values are indicative of the expected performance of the experimental apparatus, but the actual values may be somewhat different, especially for the Planck satellite.

Cosmological parameters. The validity of the Fisher matrix analysis depends on the chosen parameter set, as well as on the point \mathbf{s}_0 at which the likelihood function is supposed to reach its maximum. We use the following 9 dimensional parameter set: $\omega_b, \omega_c, \omega_{\Lambda}, \mathcal{R}, z_{eq}, n_s, n_t, r, Q$. Here n_s, n_t are the scalar and tensor spectral indices respectively, $r = C_2^T / C_2^S$ is the tensor to scalar ratio at the quadrupole, and $Q = \langle \ell(\ell+1)C_{\ell} \rangle^{1/2}$ denotes the overall normaliza-

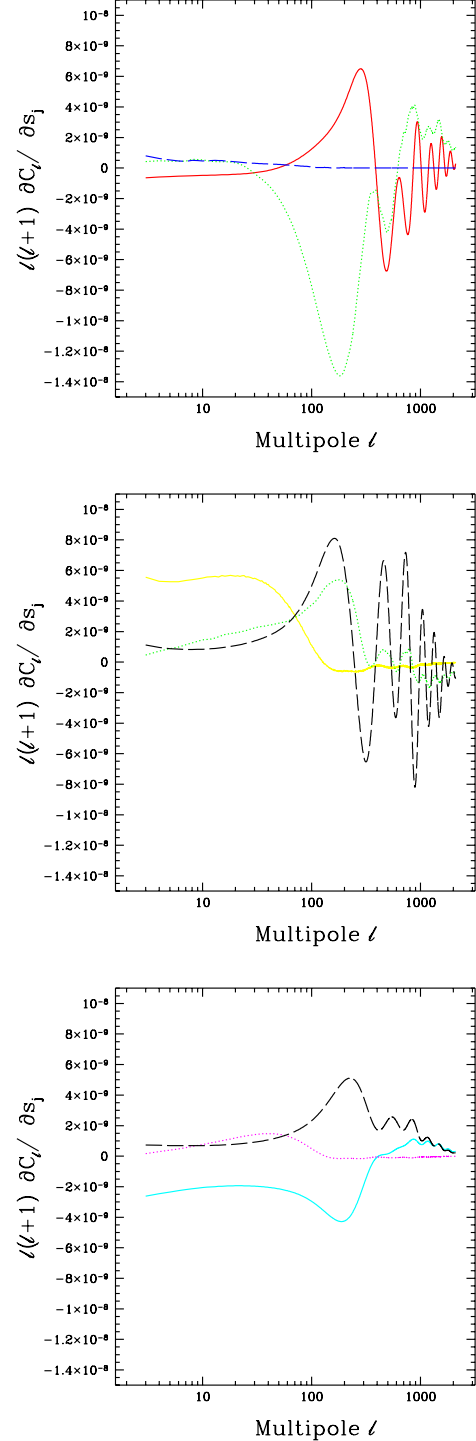


FIG. 5 — Derivatives of C_{ℓ} with respect to the 9 parameters evaluated at the reference model described in the text. The derivative $\partial C_{\ell} / \partial \omega_{\Lambda}$ has been set to 0 for $\ell > 200$ in order to suppress the effect of numerical errors, thus taking into account the geometrical degeneracy. Fig. (a): $0.1 \cdot \partial C_{\ell} / \partial \omega_b$ (red, solid); $\partial C_{\ell} / \partial z_{eq}$ (green, dotted); $\partial C_{\ell} / \partial \omega_{\Lambda}$ (blue, dashed). Fig. (b): $10 \cdot \partial C_{\ell} / \partial r$ (yellow, solid); $\partial C_{\ell} / \partial \omega_c$ (green, dotted); $\partial C_{\ell} / \partial \mathcal{R}$ (black, dashed). Fig. (c): $\partial C_{\ell} / \partial n_s$ (light blue, solid); $10 \cdot \partial C_{\ell} / \partial n_t$ (magenta, dotted); $\partial C_{\ell} / \partial Q$ (black, dashed).

	MAP				Planck			
ν (GHz)	40	60	90	100	150	220	350	
θ_c (degrees)	0.46	0.35	0.21	0.18	0.13	0.09	0.08	
$\sigma_c/10^{-6}$	6.6	12.1	25.5	1.7	2.0	4.3	14.4	
$w_c^{-1}/10^{-15}$	2.9	5.4	6.8	0.028	0.022	0.047	0.44	
ℓ_c	289	385	642	757	1012	1472	1619	
	$\ell_{max} = 1500$				$\ell_{max} = 2000$			

TABLE 1 — Experimental parameters used in the Fisher matrix analysis.

tion, where the mean is taken over the multipole range accessible to the experiment. We choose to use the shift parameter \mathcal{R} because this takes into account the geometrical degeneracy between Ω_Λ and Ω_k (Efstathiou & Bond 1999). Our purely adiabatic reference model has parameters: $\omega_b = 0.0200$ ($\Omega_b = 0.0473$), $\omega_c = 0.1067$ ($\Omega_c = 0.2527$), $\omega_\Lambda = 0.2957$ ($\Omega_\Lambda = 0.7000$), ($h = 0.65$), $\mathcal{R} = 0.953$, $z_{eq} = 3045$, $n_s = 1.00$, $n_t = 0.00$, $r = 0.10$, $Q = 1.00$. This is a fiducial, concordance model, which we believe is in good agreement with most recent determinations of the cosmological parameters (flat universe, scale invariant spectral index, BBN compatible baryon content, large cosmological constant). Furthermore, we allow for a modest, 10% tensor contribution at the quadrupole in order to be able to include tensor modes in the Fisher matrix analysis.

We plot the derivatives of C_ℓ with respect to the different parameters in Fig. 5. Generally, we remark that derivatives with respect to the combination of parameters describing the matter content of the universe (ω_b and ω_c , \mathcal{R} , z_{eq}) are large in the acoustic peaks region, $\ell > 100$, while derivatives with respect to parameters describing the tensor contribution (n_t , r) are important in the large angular scale region. Since measurements in this region are cosmic variance limited, we expect uncertainties in the latter set of parameters to be large regardless of the details of the experiment. The curve for $\partial C_\ell/\partial Q$ is of course identical to the C_ℓ 's themselves. The cosmological constant is a notable exception: variation in the value of ω_Λ keeping all other parameters fixed produces a perfect degeneracy in the acoustic peaks region. Therefore we expect the derivative $\partial C_\ell/\partial \omega_\Lambda$ to be 0 in this region. Small numerical errors in the computation of the spectra, however, artificially spoil this degeneracy, erroneously leading to smaller predicted uncertainties. In order to suppress this effect, we set $\partial C_\ell/\partial \omega_\Lambda = 0$ for $\ell > 200$. From eq. (6) we see that a large absolute value of $\partial C_\ell/\partial s_i$ leads to a large F_{ii} and therefore to a smaller $1 - \sigma$ error (roughly neglecting non-diagonal contributions). If the derivative along s_i can be approximated as a linear combination of the others, however, then the corresponding directions in parameter space will be degenerate, and the expected error will be important. This is the case for mild, featureless derivatives as $\partial C_\ell/\partial r$, while wild changing derivatives (such as $\partial C_\ell/\partial \mathcal{R}$) induce smaller errors in the determination of the corresponding parameter. Therefore the choice of the parameter set is very important in order to correctly predict the standard errors of the experiment.

Error forecast. Table 2 shows the results of our analysis for the expected $1 - \sigma$ error. Determination of the redshift of equality can be achieved by MAP with 23% accu-

	MAP	Planck
$\delta\omega_b/\omega_b$	0.116	0.005
$\delta\omega_c/\omega_c$	0.499	0.037
$\delta\omega_\Lambda/\omega_\Lambda$	3.396	1.715
$\delta\mathcal{R}$	0.008	0.001
$\delta z_{eq}/z_{eq}$	0.232	0.022
$\delta\omega_{rel}/\omega_{rel}$	0.428	0.032
ΔN_{eff}	3.170	0.237
δn_s	0.149	0.013
δn_t	1.961	1.076
$\delta r/r$	5.222	2.670
δQ	0.012	0.005

TABLE 2 — Fisher matrix analysis results: expected $1 - \sigma$ errors for the MAP and Planck satellites. See the text for details and discussion.

racy, while Planck will pinpoint it down to 2% or so. From $\omega_{rel} = (\omega_b + \omega_c)/z_{eq}$ it follows that the energy density of relativistic particles, ω_{rel} , will be determined within 43% by MAP and 3% by Planck. This translates into an impossibility for MAP of measuring the effective number of relativistic species ($\Delta N_{eff} \approx 3.17$ at 1σ), while Planck will be able to track it down to $\Delta N_{eff} \approx 0.24$. As for the other parameters, while the acoustic peaks' position (through the value of \mathcal{R}) and the matter content of the universe can be determined by Planck with high accuracy (of the order of or less than one percent), the cosmological constant remains (with CMB data only) almost undetermined, because of the effect of the geometrical degeneracy. The scalar spectral index n_s and the overall normalization will be well constrained already by MAP (within 15% and 1%, respectively), while because of the reasons explained above the tensor spectral index n_t and the tensor contribution r will remain largely unconstrained by both experiments. Generally, an improvement of a factor 10 is to be expected between MAP and Planck in the determination of most cosmological parameters. Our analysis considers temperature information only, while it is well known that inclusion of polarization measurements greatly improves determination of the tensor mode parameters (see e.g. Bucher et al. 2000). For Planck, which will have polarization measurement capabilities, this will be of great importance.

A Fisher matrix analysis for ΔN_{eff} was previously performed by Lopez et al. (1999) and repeated by Kinney & Riotto (1999) (with the equivalent chemical potential ξ), and a strong degeneracy was found between N_{eff} , h and Ω_Λ , and to lesser extent with Ω_b . We have seen here that the degeneracy really is between ω_{rel} , ω_m and n , and the degeneracy previously observed is thus explained because they considered flat models, where a change in Ω_Λ is equivalent to a change in ω_m , $\omega_m = (1 - \Omega_\Lambda - \Omega_b)h^2$. The results of this paper, on how precisely the future satellite missions can extract the relativistic energy density, can be translated into approximately $\Delta N_{eff} = 3.17$ ($\xi = 2.4$) and $\Delta N_{eff} = 0.24$ ($\xi = 0.73$) for MAP and Planck respectively.

6 CONCLUSIONS

In this paper, we have examined the effect of varying the background of relativistic particles on the cosmological parameters derived from CMB observations. We have found that the present constraints on the overall curvature, Ω_k , and tilt of primordial fluctuations, n_s , are slightly affected by the inclusion of this background. However, we have found a relevant degeneracy with the amount of non relativistic matter ω_m . Even with relatively strong external priors (flatness, $h = 0.65 \pm 0.2$, age > 10 Gyrs) the present CMB bound (95% c.l.) $0.1 < \omega_m < 0.2$ spreads to $0.05 < \omega_m < 0.45$ when variations in ω_{rel} are allowed. Specifically, without priors on ω_m (through flatness, h , etc) no bounds on N_{eff} can be obtained.

Another fundamental point bears on the identification of the best choice of parameters, i. e. parameter combinations which can be unambiguously extracted from CMB data. It is of the greatest importance to realize which parameter set is least plagued by degeneracy problems, i. e. which directions in parameter space are non-flat. In the well known case of the geometrical degeneracy, the shift parameter \mathcal{R} can be determined with very high precision by measuring the position of the peaks. The curvature and the Hubble parameters, however, are almost flat directions in parameter space, and therefore are not ideal variables for extraction from CMB data. In this work, we have pointed out that an analogous situation exists for z_{eq} , ω_{rel} and ω_m . In fact, z_{eq} is well determined because it measures the physical distance to equality time, while on the contrary ω_m is a rather ill-suited variable for CMB data, since it suffers from degeneracy with ω_{rel} (at least up to the third acoustic peak).

Fortunately, as we saw in the last section, the matter – radiation degeneracy in the CMB data is present only up to the third peak and future space missions like Planck will be able to determine separately the amount of matter and radiation in the universe.

ACKNOWLEDGMENTS

We thank Celine Boehm, Ruth Durrer, Louise Griffiths and Alain Riazuelo for useful comments. RT is grateful to the University of Oxford for the hospitality during part of this work. RB is supported by the Fitzgerald Scholarship fund. SHH is supported by a Marie Curie Fellowship of the European Community under the contract HPMFCT-2000-00607. AM is supported by PPARC. This work is supported by the European Network CMBNET.

REFERENCES

Albrecht A., Skordis C., 2000, Phys. Rev. Lett. 84, 2076
 Amendola L., Gordon C., Wands D., Sasaki M., 2001, preprint (astro-ph/0107089)
 Bahcall N. et al., astro-ph/0002310.
 Baltz E., Gondolo P., 2001, preprint (hep-ph/0105249)
 Barger V., Kao C., 2001, preprint (hep-ph/0106189)
 Bartlett J. G., Hall L. J., 1991, Phys. Rev. Lett. 66, 541
 Bean R., Hansen S. H., Melchiorri A., 2001, preprint (astro-ph/0104162)
 Beaudet G., Goret P., 1976, Astron. & Astrophys., 49, 415
 de Bernardis P. et al., 2000, Nature, 404, 955

Bond R.J., Efstathiou G., Tegmark M., 1997, MNRAS, preprint (astro-ph/9702100)
 Bond J. R., Jaffe A. H., 1998, preprint (astro-ph/9809043)
 Bouchet F. R., Peter P., Riazuelo A., Sakellariadou M., 2000, preprint (astro-ph/0005022)
 Bucher M., Moodley K., Turok T., 2000, preprint (astro-ph/0012141)
 Burles S., Nollett K. M., Truran J. N., Turner M. S., 1999, Phys. Rev. Lett. 82, 4176
 Carlberg R.G. et al., astro-ph/9612169.
 Croft R. A. C. et al., 2000, preprint (astro-ph/0012324)
 Dicus D. A., Kolb E. W., Gleeson A. M., Sudarshan E. C., Teplitz V. L., Turner M. S., 1982, Phys. Rev. D, 26, 2694
 Djouadi A., Drees M., Kneur J.L., 2001, preprint (hep-ph/0107316)
 Dolgov A. D., Hansen S. H., Semikoz D. V., 1997, Nucl. Phys. B, 503, 426
 Dolgov A. D., Hansen S. H., Semikoz D. V., 1998, Nucl. Phys. B, 524, 621
 Dolgov A. D., Hansen S. H., Semikoz D. V., 1999, Nucl. Phys. B, 543, 269
 Dolgov A. D., Hansen S. H., 2001, preprint (hep-ph/0009083)
 Durrer R., Kunz M., Melchiorri A., 2001, Phys. Rev. D, 63, 081301
 Efstathiou G., Bond J. R., 1999, MNRAS, 304, 75
 Efstathiou G., 2001, preprint (astro-ph/0109151)
 Efstathiou G. et al. (2dFGRS Team), 2001, preprint (astro-ph/0109152)
 Eisenstein D. J., Hu W., Tegmark M., 1998, preprint (astro-ph/9805239)
 Ellis J. R., Nanopoulos D. V., Olive K. A., 2001, Phys. Lett. B, 508, 65
 Esposito S., Miele G., Pastor S., Peloso M., Pisanti O., 2000, Nucl. Phys. B590, 539
 Esposito S., Mangano G., Melchiorri A., Miele G., Pisanti O., 2001, Phys. Rev. D, 63, 043004
 Fogli G. L., Lisi E., Marrone A., Montanino D., Palazzo A., 2001, preprint (hep-ph/0104221)
 Garnavich P. M. et al., 1998, Ap.J., 493, L53
 Gonzalez-Garcia M. C., Maltoni M., Pena-Garay C., Valle J. W. F., 2001, Phys. Rev. D, 63, 033005
 Griffiths L. M., Silk J., Zaroubi S., 2000, preprint (astro-ph/0010571)
 Halverson N. W. et al., 2001, preprint (astro-ph/0104489)
 Hamilton A. J. S. & Tegmark M., 2000, MNRAS in press, [astro-ph/0008392]
 Hannestad S., 2000, Phys. Rev. Lett. 85, 4203
 Hannestad S., 2001, Phys. Rev. D, 64, 083002
 Hannestad S., Hansen S. H., Villante F. L., Hamilton A. J., 2001, preprint (astro-ph/0103047)
 Hansen S. H., Villante F. L., 2000, Phys. Lett. B, 486, 1
 Hansen S. H., Mangano G., Melchiorri A., Miele G., Pisanti O., 2001, preprint (astro-ph/0105385)
 Heckler A. F., 1994, Phys. Rev. D, 49, 611
 Hu W., Eisenstein D. J., Tegmark M., White M. J., 1999, Phys. Rev. D, 59, 023512
 Kang H., Steigman G., 1992, Nucl. Phys. B, 372, 494
 Kinney W., Melchiorri A., Riotto A., 2000, Phys.Rev. D63 (2001) 023505, [astro-ph/0007345].
 Kinney W. H., Riotto A., 1999, Phys. Rev. Lett. , 83, 3366
 Kneller J. P., Scherrer R. J., Steigman G., Walker T. P., 2001, preprint (astro-ph/0101386)
 Knox L., 1999, Phys. Rev. D, 52, 4307
 Kolb E. W., Turner M. S., Chakravorty A., Schramm D. N., 1991, Phys. Rev. Lett. 67, 533
 Langacker P., 1989, UPR-0401T
 Lee A. T. et al., 2001, preprint (astro-ph/0104459)
 Linde A. D., 1990, Particle Physics And Inflationary Cosmol-

- ogy, (Chur, Switzerland: Harwood, Contemporary concepts in physics, 5)
- Lisi E., Sarkar S., Villante F. L., 1999, *Phys. Rev. D*, 59, 123520
- Lopez R. E., Dodelson S., Heckler A., Turner M. S., 1999, *Phys. Rev. Lett.* 82, 3952
- Lopez R. E., Turner M. S., 1999, *Phys. Rev. D*, 59, 103502
- MAP, see webpage <http://map.gsfc.nasa.gov/>
- Melchiorri A. et al, *Astrophys.J.* 536 (2000) L63
- Melchiorri A., Griffiths L. M., 2001, *New Astronomy Reviews*, 45, Issue 4-5
- Netterfield C. B. et al., 2001, preprint (astro-ph/0104460)
- Orito M., Kajino T., Mathews G. J., Boyd R. N., 2000, preprint (astro-ph/0005446)
- Percival W. J. et al., 2001, preprint (astro-ph/0105252)
- Planck, see webpage <http://astro.estec.esa.nl/Planck>
- Pryke C., Halverson N. W., Leitch E. M., Kovac J., Carlstrom J. E., Holzzapfel W. L., Dragovan M., 2001, preprint (astro-ph/0104490)
- Perlmutter S. et al., 1997, *Ap. J.*, 483, 565
- Perlmutter S. et al. [Supernova Cosmology Project Collaboration], 1999, *Astrophys. J.* 517, 565
- Santos M. G. et al., 2001, preprint (astro-ph/0107588)
- Seljak, U., Zaldarriaga M., 1996, *Ap.J.*, 469, 437
- Seljak U., Zaldarriaga M., 1996, *Phys. Rev. Lett.*, 78, 2054
- Saunders W. et al., 2000, *Mon. Not. R. Astron. Soc.*, 317, 55
- Skordis C., Albrecht A., 2001, preprint (astro-ph/0012195)
- Steigman G., 2001, preprint (astro-ph/0108148)
- Tegmark M., Zaldarriaga M., Hamilton A. J., 2001, *Phys. Rev. D*, 63, 043007
- Trotta R., Riazuelo, A., Durrer R., 2001, *Phys. Rev. Lett.* (in press)
- Wang X., Tegmark M., Zaldarriaga M., 2001, preprint (astro-ph/0105091)
- Weller J. & Albrecht A., astro-ph/0106079.
- White M., Gelmini G., Silk J., 1995, *Phys. Rev. D*, 51, 2669
- Zentner A. R., Walker T. P., 2001, preprint (astro-ph/0110533)